Modularized Field-Effect Transistor Biosensors

Xiaochuan Dai[†], Richard Vo[†], Huan-Hsuan Hsu, Pu Deng, Yixin Zhang, and Xiaocheng Jiang[*]

Department of Biomedical Engineering, Tufts University, Medford, Massachusetts, 02155, United States

ABSTRACT

Field-effect transistors (FETs), when functionalized with proper bio-recognition elements (such as antibodies or enzymes), represent a unique platform for real time, specific, label-free transduction of biochemical signals. However, direct immobilization of bio-recognition molecules on FETs imposes limitations on re-programmability, sensor regeneration and robust device handling. Here we demonstrate a modularized design of FET biosensors with separate bio-recognition and transducer modules, which are capable of reversible assembly and disassembly. In particular, hydrogel "stamps" immobilizing bio-receptors have been chosen to build bio-recognition modules to reliably interface with FET transducers structurally and functionally. Successful detection of penicillin down to 0.25 mM has been achieved with penicillinase-encoded hydrogel module, demonstrating effective signal transduction across the hybrid interface. Moreover, sequential integration of urease- and penicillinase-encoded modules on the same FET device allows us to reprogram sensing modality without cross-contamination. In addition to independent bio-receptor encoding, the modular design also fosters sophisticated control of sensing kinetics by modulating the physiochemical microenvironment in the bio-recognition modules. Specifically, the distinction in hydrogel porosity between polyethylene glycol and gelatin enables controlled access and detection of larger molecules, such as poly-L-lysine (MW 150-300 kDa), only through the gelatin module. Bio-recognition modules with standardized interface designs have also been exploited to comply with additive mass fabrication by 3D printing, demonstrating potential for low cost, ease of storage, multiplexing and great customizability for personalized biosensor production. This generic concept presents a unique integration strategy for modularized bioelectronics and could impact broadly hybrid device development.

KEYWORDS

Bioelectronics / hydrogel-gate / modular design / programmable / customizable / mass production

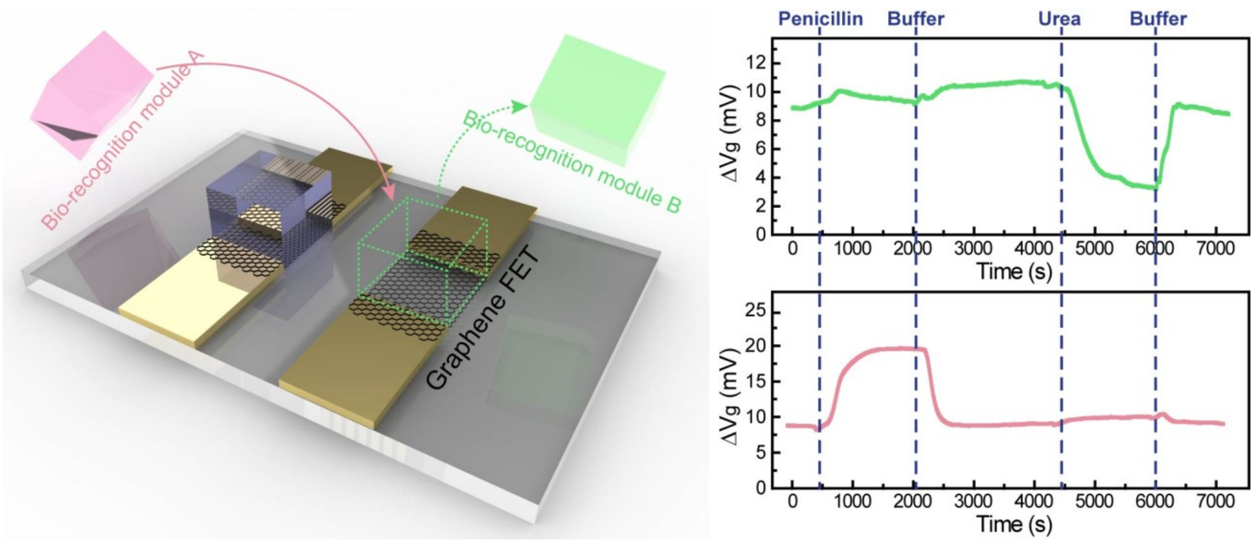

Rapid progress in biosensor development has led to innumerous technological advances in healthcare research and impacted important clinical applications[1,2]. Field-effect-transistor (FET) based biosensors represent a unique class of analytical tools for label-free specific detection of bio-analytes with unprecedented sensitivity[3-6], fast response time[7,8], potential for miniaturization and multiplexing[3,9], as well as facile integration with developed semiconductor electronics technologies[4,10]. Specific sensing with FET biosensor involves structural and functional integration of bio-recognition molecules, such as enzymes, antibodies, aptamers, etc., with FETs, where the selective interaction between bio-analytes and bio-receptors could result in biophysical or biochemical changes that can be further transduced and amplified via field effect towards external signal readouts[3,6,10,11]. For example, enzyme functionalized FET biosensors can react with specific substrates, where the enzymatic transformation leads to perturbation of electric potential at the FET channel/electrolyte interface and induces a change of the charge carrier density and the conductance of FET devices as readouts in real time[10,12]. Similarly, antibody functionalized FET biosensor may specifically bind to the corresponding antigen molecules. Because most biomolecules carry electrostatic charges (or can carry electrostatic charges at suitable pH), such binding events will also lead to local electric potential change at the surface of FET channels[3,6,11,13].

However, the bio-recognition elements are commonly immobilized directly in close proximity on the FET channel/electrolyte interface via physical absorption or chemical conjugation for efficient signal coupling[3,13-15]. This is especially critical for detection in physiologically relevant environments where the chemical "outputs" from enzymatic reactions will be quickly diluted and/or neutralized, while the electric field generated by charged analytes will also diminish at distance of nanometer scale as a result of enhanced electrostatic screening in high ionic strength solutions, known as Debye screening[15,16]. Such demanded structural intimacy between bio-recognition and FET elements in traditional FET biosensors has largely limited the design versatility and translational applications. For example, re-programming the sensing specificity to detect different target molecules is often difficult or requires complicated and time consuming steps after the initial functionalization. Additionally, after sensing tests are performed, it lacks versatile methods to regenerate the sensing capability of the receptors without compromising the functionality of the bio-receptor[17] especially ones that irreversibly bind to target with a high affinity coefficient. Moreover, the bio-receptor functionalization process must be compatible with post-fabricated FETs and the stability of bio-receptors in sensing solutions limits the life-time of the hybrid device[18]. A modular design of FET biosensors, consisting of separate electronic and bio-recognition elements capable of reversible assembly and disassembly has the potential to overcome these limitations (**Figure 1a**), yet challenges remain to formulate an inter-module interface that can simultaneously allow for effective signal coupling when integrated and free of cross-contamination once dissembled/re-assembled.

To this end, the design and construction of bio-recognition module needs to fulfill the following criteria: (1) the bio-recognition module has to structurally support the robust immobilization and handling of bio-receptors; (2) the bio-recognition module should allow open access of biochemical "inputs" (i.e., the analyte molecules); (3) the "outputs" from bio-recognition modules need to be effectively coupled to and reliably transduced by the FET module. Functional hydrogel represents ideal backbone material for the bio-recognition modules to enable seamless structural and functional integration with FET transducers. By creating a confined microenvironment with tunable diffusion barriers, it offers controlled access to biochemical "inputs" and highly localized enrichment/amplification of biochemical "outputs" before they get diluted/neutralized by the buffer (**Figure 1a**). It has also been demonstrated to modulate the local dielectrics to mitigate Debye screening thus enabling charged based sensing in high ionic strength solutions[12]. These amplified biochemical and/or charge signals are critically important to the reliable signal transduction across the modular interface (**Figure 1b**). It is worth noting that the bio-recognition module can grant possibility for modulating selective accessibility or controlled diffusion dynamics of specific "input" through porosity engineering as well as rationally designed matrices properties. Additionally, the excellent structural integrity and biocompatibility of hydrogel matrices allow the bio-recognition modules to be independently designed, manufactured and preserved with significantly improved scalability and shelf-life[12,18]. The unitary design of the bio-recognition module may allow for more complex bio-recognition modules with spatial organization and integration over multiple biological processes, such as enzymatic cascades for intricate biosensing. Through reversible assembly and disassembly of diverse bioactive hydrogel modules with FET modules, the two-step tandem signal transduction can be easily connected and disconnected on demand to achieve re-programmable sensing capabilities.

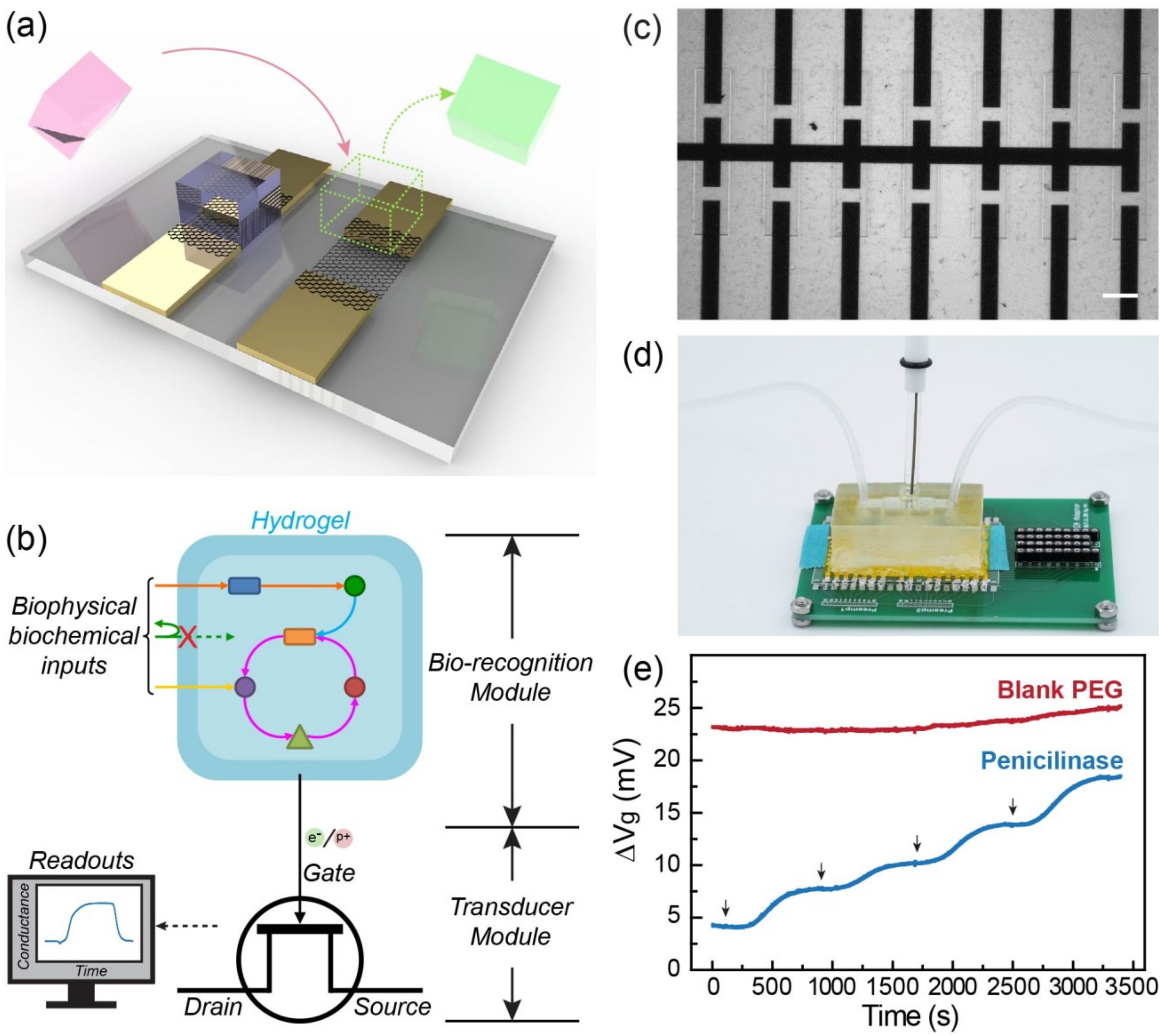

Figure 1. Modularized FET biosensor (a) Schematic representation of modularized graphene FET biosensor with reversibly assembled and dissembled bio-recognition modules (pink, green and

blue cubes). Gold, electrode interconnects for the graphene FET devices. Black, graphene channels. (b) Diagram showing stitched two step signal transduction in bio-recognition module and FET transducer module, respectively, enabled by modularized FET biosensors. Squares, triangles, circles and colored arrows conceptually denote biologically relevant processes undergoing in hydrogel bio-recognition module. (c) Optical image of graphene FET arrays protected with S1813 photoresist which will be removed with acetone before used for sensing. Dark lines are evaporated Cr/Au interconnects. Scale bar, 200 μm. (d) Photograph of the device chip. Cr/Au interconnects are connected to printed circuit board with silver paste and then wired to the data acquisition systems through receptacle connector arrays. A 3D printed fluidic channel is aligned and attached onto the center of the device chip. Silicone inlet and outlet tubing are inserted. Ag/AgCl electrode was placed into the channel as reference electrode. (e) Real time penicillin sensing. Blue and red traces represent recording from FET biosensors integrated with penicillinase-encoded receptor module and blank hydrogel module, respectively. Arrows depict the time points chronologically of solution switching to phosphate buffer with 0.25 mM, 0.5 mM, 1.0 mM and 2.0 mM penicillin.

For proof-of-concept demonstration, graphene was chosen as channel material for fabricating the FET modules. Specifically, single layer graphene synthesized on copper foil catalyst via chemical vapor deposition was transferred onto photolithographically patterned gold electrodes and configured as FET channels (**Figure 1c**)[12]. Bioactive enzymes, such as penicillinase and urease, are PEGylated and co-polymerized with polyethylene glycol diacrylate (PEGDA)[19] to create hydrogel "stamps" as bio-recognition modules. After mounting the FET sensing chip onto printed circuit board with receptacle connectors, a 3D printed chamber with configured fluidic channel was aligned and mounted on the FET sensing chip (**Figure 1d**)[20]. Inlet/outlet tubing and Ag/AgCl reference electrode were then connected onto the fluidic channel for delivery of analytes solutions and buffers as well as applying electrolyte gate, respectively (**Figure 1d**)[20]. The encoded hydrogels "stamps" (bio-recognition module) were placed in direct contact with the graphene channels (transducer module) to complete the assembly of FET biosensors with respective sensing modalities. Following the connection of FET sensing chip to the data acquisition system, real time electrical characterization of FET biosensor and the sensing experiments were performed by continuously recording the conductance of individual FET devices while introducing analyte solutions or buffers in desirable sequence via the inset/outlet tubes. **Figure S1** shows a representative conductance variation as a function of electrolyte-gate voltage for graphene FET, with clear bipolar transconductance on each side from Dirac point[13,21,22].

To investigate the effectiveness of signal coupling and transduction across the separate modules, we have demonstrated the detection of penicillin G using penicillinase-encoded hydrogel as the bio-recognition module. Penicillinase catalyzes the hydrolysis of penicillin into penicilloic acid, releases protons and therein leads to a decrease of the local pH, which is then transduced and detected as a decrease in conductance via field effect[10]. Based on the electrolyte-gate measurement of the graphene FET (**Figure S1**), sensing signal amplitude was calculated by dividing the conductance change with the transconductance value at V_g of the sensing tests. **Figure 1e** shows the real time recording of signal amplitude while sequentially switching the 5 mM phosphate buffer with various concentration of penicillin G from 0.25 mM to 0.5 mM, 1.0 mM and 2.0 mM[23], demonstrating the concentration dependent detection (**Figure 1e**, blue curve). The detection amplitude and limit of detection (**Figure S2**) are consistent with hydrogel-gate FET biosensor where hydrogel is directly photopolymerized on top of graphene FETs, presenting the uncompromised signal transduction across two modules[12]. In clear comparison, stable conductance was recorded from another FET biosensor assembled with a blank PEG hydrogel module as a control experiment (**Figure 1e**, red curve), demonstrating the signal coupling is well-confined within the hydrogel bio-recognition modules which is critical for potential multiplexing biosensors.

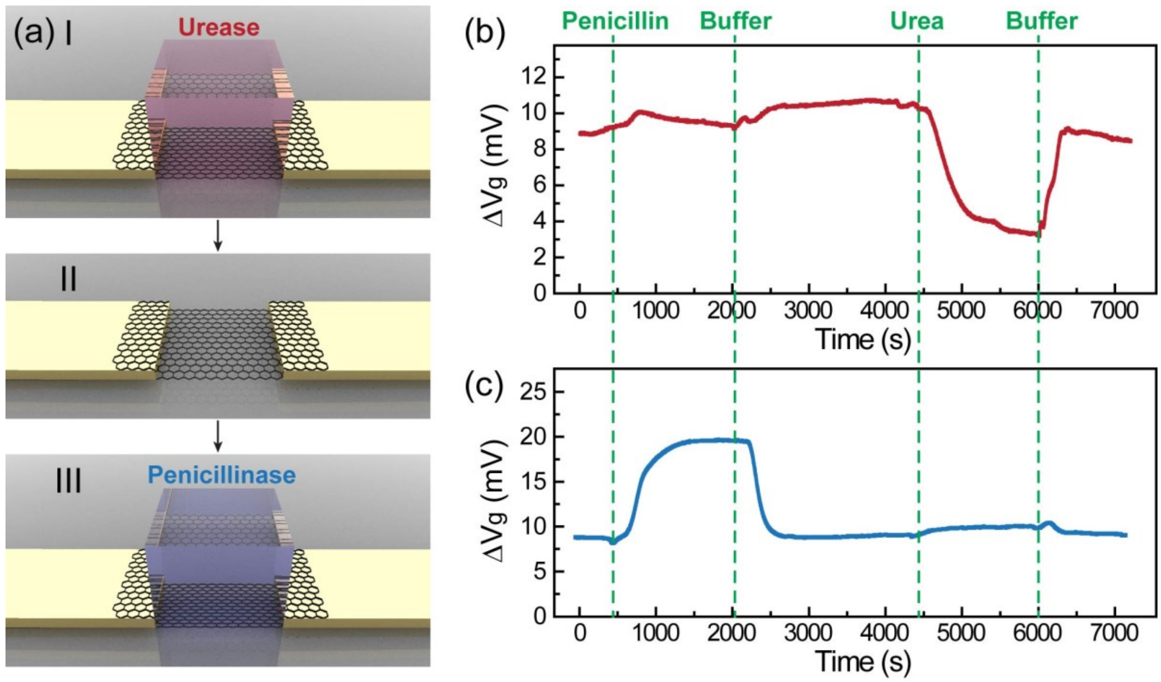

Figure 2. Switchable module (a) Schematic of switching bio-recognition modules from urease-encoded (red) to penicillinase-encoded (blue) PEG. (b-c) Real time recording from the FET biosensors integrated with urease-encoded (red trace) and penicillinase-encoded bio-recognition module (blue trace), respectively. Green dashed lines indicate the time points chronologically of solution switching to phosphate buffer with 1.0 mM penicillin, pure phosphate buffer, phosphate buffer with 1.0 mM urea and pure phosphate buffer.

The modularization of FET biosensor also allows us to freely connect and disconnect the signal coupling between the bio-recognition and transducer modules and, as a result, switch the sensing modalities of the same FET transducer. As a proof of the concept, we choose urease-encoded bio-recognition module in addition to penicillinase to demonstrate the capability of re-programming the modularized FET biosensors. Urease catalyzes the hydrolysis of urea to generate ammonium, which will lead to an increase of the local pH and an increase in conductance of the measured device[24]. First, the urease-encoded bio-recognition module was integrated onto the FET transducer (**Figure 2a**, I). When 5 mM phosphate buffers containing 1 mM penicillin, no analyte, 1 mM urea and no analyte[23] were sequentially introduced, highly specific signal corresponding to urea injection was recorded with minimal nonspecific signal from penicillin (**Figure 2b**). Following the sensing test, urease-encoded bio-recognition module was detached from the FET devices and a similar penicillinase-encoded bio-recognition module was then assembled onto the same FET device (**Figure 2a**, II and III). Sensing experiment with same analyte solutions introduced at the same order was repeated. Specific detection of penicillin was achieved and no signal was observed this time following urea injection (**Figure 2c**), demonstrating the successful reprogramming of the modularized FET biosensor and that the disconnection of urease bio-recognition module doesn't leave any cross-contamination. The integration and disintegration of bio-recognition modules has been repeated over 35 times, and the recorded signal amplitudes are consistent between multiple switching, indicating the reproducibility and stability among module switches (**Figure S3**). This reprogrammability feature can also foster unique applications FET biosensor that involves irreversible bio-recognition process, such as detection of antibody-antigen binding kinetics, where regeneration of the devices can be conveniently achieved via replacement of fresh bio-recognition modules. This discovery has extensively broadened our flexibility to design and fabricate both recognition and transducer modules independently for specific tuning requirement and eventually achieve biosensor with multifunctionalities by integrating various kinds of modules.

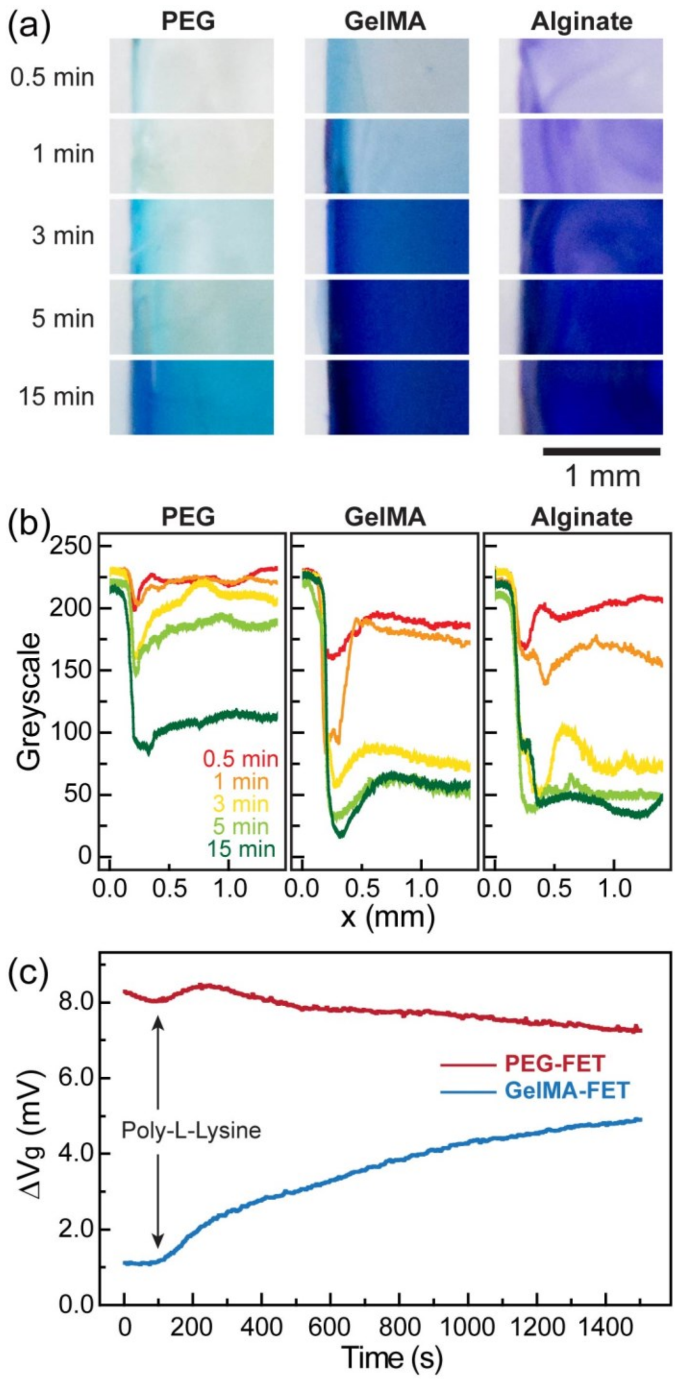

Figure 3. Material versatility (a) Photographs showing diffusion of methylene blue into PEG, gelatin and alginate hydrogels for 0.5, 1, 3, 5, and 15 minutes. The vertical white/blue color transition aligned to approximately one-sixth of each panels indicates the boundary of hydrogels. (b) Quantitatively analysis of greyscale profiles across each of the panels in (a), indicating time dependent diffusion of methylene blue into PEG, gelatin and alginate hydrogels. All the traces are averaged from 5 horizontal cross sections evenly distributed. (c) Real time recording from FET

biosensors integrated with receptor module composed of PEG (red trace) and gelatin (blue trace), respectively. Arrow indicates the time point of solution switching to phosphate buffer containing 0.005% (w/v) poly-l-lysine.

In addition to the capability to customize and switch the bio-receptor encoding in the bio-recognition modules, the structural and functional properties of the hydrogel microenvironment can also be independently fabricated and customized to meet various sensing requirements. For example, hydrogels with controlled porosities could allow us to control the diffusion dynamics[25] of analytes with different molecular weights; the tunable chemical properties of the hydrogels could also enable selective accessibility of molecules with certain charges or chemical affinity[26]; likewise hydrogel capable of degrading or phase transition[27] could be utilized to make transient or switchable biosensors; and more. To prove our concept, we chose three commonly used hydrogel materials, PEGDA, gelatin methacryloyl (GelMA) and alginate, with significantly different porosity to demonstrate the modulation of the mass transport across the hydrogel matrices[25,28,29]. Specifically, polymerized hydrogel "stamps" composed of PEG, gelatin and alginate[30] were placed in a solution of 1 mM methylene blue (MW 320 g/mol) and collected after 0.5, 1, 3, 5 and 15 min for imaging. **Figure 3a** shows the distinct diffusion behavior of methylene blue into different hydrogel "stamps" from solution interface over time. Quantitative analysis (**Figure 3b**) of the color changes was carried out by plotting the greyscale profiles horizontally across each panel from **Figure 3a**. It is clear to see that minimal changes in color occur after 5 min exposure of gelatin and alginate to methylene blue, at which condition the diffusion of methylene blue could be treated as saturation (~100%). Normalized by the saturation assumption, gelatin and alginate already exhibit 84% and 86% saturation after 3 min exposure to methylene blue, respectively. However, PEG hydrogel only reaches 56% saturation even after being exposed to methylene blue for 15 min. The different diffusion rate in these hydrogels can be attributed to the variation of the pore size between PEG, gelatin, and alginate. Crosslinking of small-molecular weight PEGDA (MW 575 g/mol) has been shown to have nanometer scale pore size[25], as compared to micrometer for GelMA[28] and alginate[29], while fine tuning of the pore size can also be achieved by co-polymerization of desirable porogens[31,32].

The difference in porosity has been utilized to tune and optimize sensing kinetics between analytes with distinct molecular weights, which has the potential to supplement additional selectivity when processing complex physiological fluids such as blood, saliva, urine, etc. PEG hydrogel-gate has been shown to eliminate absorption and detection of large molecular bovine serum albumin limited by its intrinsic small pore size[12]. Here, poly-L-lysine (PLL, MW $1.5-3.0\times10^5$ g/mol) was tested in parallel with FET biosensors integrated with gelatin and PEG modules, to evaluate the effect of hydrogel pore size on analyte accessibility. Simultaneous recording from gelatin-FET and PEG-FET biosensors was performed while 0.005 % (w/v) PLL in 5 mM phosphate buffer[23] was introduced. An approximate 4 mV signal was observed due to the nonspecific binding of positively charged PLL only from gelatin-FET device whereas no signal was detected from the PEG-FET (**Figure 3c**). Moving forward, selectivity with different requirements can be achieved by more sophisticated structural and compositional modulation of the receptor module backbone[33,34].

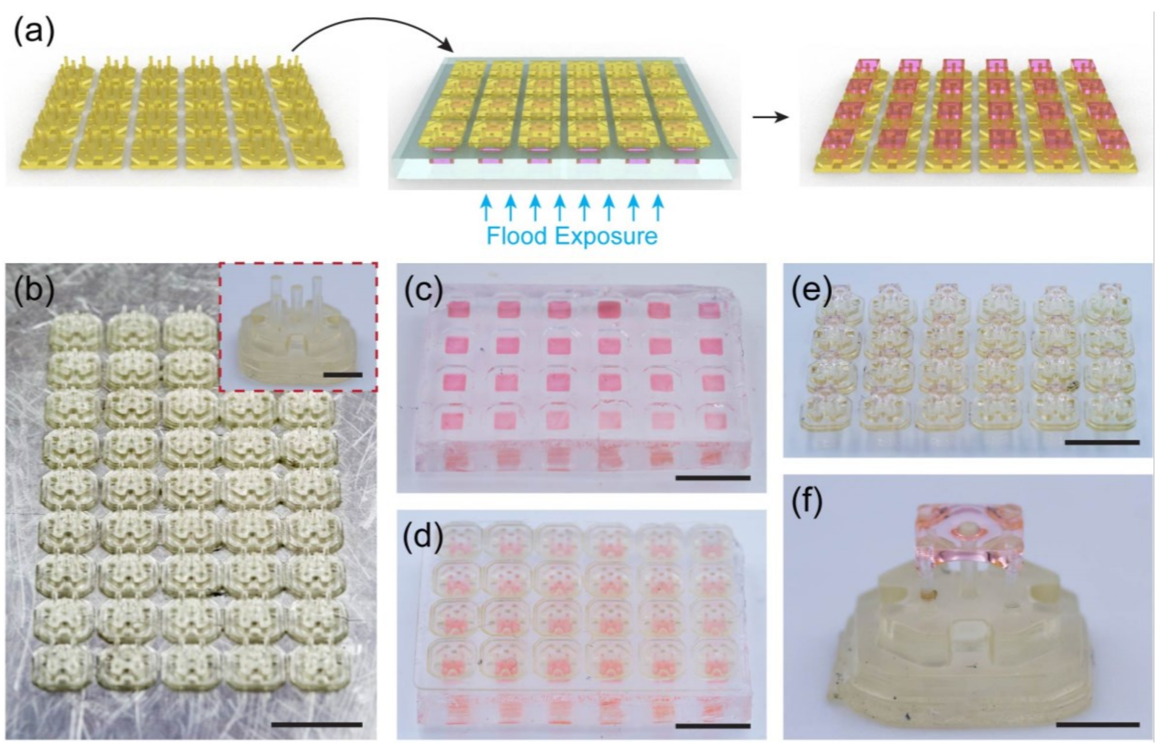

Figure 4. Additive manufacturing (a) Schematic showing the process of mass fabrication of an array of hydrogel receptor modules. (b) Photograph of “stamps” used for picking up thin hydrogels

and interface with FET modules via standard sockets, printed en masse on stereolithography 3D printer building plate. Scale bar, 10 mm. Inset, a high magnification photograph of individual “stamp”. Scale bar, 2 mm. (c) Photograph of hydrogel monomer solution in PDMS wells. Scale bar, 10 mm. (d) Photograph of an array of 3D printed “stamp” placed into PDMS wells. Scale bar, 10 mm. (e) Photograph of an array of fabricated receptor modules. Scale bar, 10 mm. (f) A high magnification photograph of an individual receptor module, highlighting thin hydrogel held by several pillars on the “stamp” and standard socket used for interface with the FET transducers. Scale bar, 2 mm.

Stemming from modular design, we have demonstrated the capability to independently customize the bio-recognition modules with precise control over both active (bio-receptors) and passive (microenvironment) components. The design and processing is inherently compatible with additive manufacturing techniques, such as 3D printing, to construct a customizable interface for module integration, low cost and high material efficiency, ease of fabrication and mass production[35]. As shown schematically in **Figure 4a**, the bio-recognition modules adopted in our tests could be mass produced by 3D printing in batches, followed by photopolymerization of hydrogels in a large array. Specifically, 3D printing was first used to fabricate the “stamps” designed with (1) standardized LEGO™-like docking structure to facilitate the “plug-and-play” integration to FET module attached with complementary structure, and (2) an array of pillars to pick up the hydrogel elements (**Figure 4b**). After 3D printing, the “stamps” were cleaned with ethanol and UV-cured for 30 minutes. Polydimethylsiloxane (PDMS) mold casted with same pitches was made to create mini-wells holding hydrogel monomer solution (**Figure 4c**) and then interfaced with the pillar side of the “stamps” (**Figure 4d**). Following the light exposure of 1 min, array of “stamps” could be detached from the PDMS wells with a thin piece of hydrogel elements picked up by the pillar structure, the “stamp” modules with hydrogel elements could be easily integrated with the FET devices or stored for later use (**Figure 4e** and **4f**). 3D printing allows for low cost, high throughput fabrication, and compared to traditional functionalization methods, polymerization step requires as little as 4 μL monomer solution to fabricate a hydrogel-equipped “stamp” capable of covering 2×2 mm^2, and can make 100% use of the bio-receptor molecules. This generic strategy is not limited to photopolymerization and can be customized for different categories of material processing such as gelation of gelatin and agarose through temperature-mediated phase transition[36]. This strategy should also not be limited to enzyme-based biosensors but can be expanded to other bio-recognition elements such as single stranded DNA, antibodies, aptamers, etc. These methods may require additional optimization of the hydrogel microenvironment for optimal signal transduction. Significantly, granted by the simple "plug-and-play" integration and standardized interface, a large pool of bio-recognition modules fabricated by different bio-receptors and matrix materials can be pre-formulated and stored as bioactive "cartridges" for potential customizable assembly of modularized FET biosensors upon usage, showing its great potential for low cost personalized multifunctional point-of-care biosensor tool kit.

In conclusion, we outline a novel and general strategy to fabricate modularized FET biosensor consisted of independently customized hydrogel "stamps" as bio-recognition modules and graphene FETs as transducer modules. The modular design has been exploited to enable real time, label-free detection of penicillin G and urea with penicillinase- and urease-encoded PEG hydrogel as bio-recognition modules, respectively. Additionally, the modular design allows us to freely assemble and disassemble FET transducer module with a variety of bio-recognition modules composed of different hydrogel materials, different bio-receptors, etc. to achieve a number of different purposes in sensing tests. The modularization also offers standardized preparation of bio-recognition modules for customizability, low cost, mass production. The modularized design and facile integration of hydrogel "stamps" and graphene FETs has demonstrated functional integration of bio-recognition modules and transducer modules in biochemical sensing and could lead to broadly functional integration of biological- (in biomaterials) and electronic- (in solid-state) transducers for many new possibilities in hybrid device development[37-39]. We anticipate this strategy will lead to improvements in FET biosensors for applications such as point-of-care diagnostics and personalized medicine[40-42].

ASSOCIATED CONTENTS

Supporting Information

Additional information including figures showing device design, measurement setup and liquid gate measurement.

AUTHOR INFORMATION

Corresponding Author

*Email: Xiaocheng.Jiang@tufts.edu.

Author Contributions

† X.D. and R.V. contributed equally to this work.

Notes

The authors declare no competing financial interest.

ACKNOWLEDGMENT

The authors greatly acknowledge support from National Science Foundation (NSF CBET-1803907) and Air Force Office of Scientific Research (FA9550-18-1-0128).

REFERENCES

(1) Chen, A. C.; Chatterjee, S. Nanomaterials based electrochemical sensors for biomedical applications. *Chem. Soc. Rev.* **2013**, *42*, 5425-5438.

(2) Kim, J.; Campbell, A. S.; de Avila, B. E. F.; Wang, J. Wearable biosensors for healthcare monitoring. *Nat. Biotechnol.* **2019**, *37*, 389-406.

(3) Zheng, G. F.; Patolsky, F.; Cui, Y.; Wang, W. U.; Lieber, C. M. Multiplexed electrical detection of cancer markers with nanowire sensor arrays. *Nat. Biotechnol.* **2005**, *23*, 1294-1301.

(4) Stern, E.; Klemic, J. F.; Routenberg, D. A.; Wyrembak, P. N.; Turner-Evans, D. B.; Hamilton, A. D.; LaVan, D. A.; Fahmy, T. M.; Reed, M. A. Label-free immunodetection with CMOS-compatible semiconducting nanowires. *Nature* **2007**, *445*, 519-522.

(5) Hahm, J.; Lieber, C. M. Direct ultrasensitive electrical detection of DNA and DNA sequence variations using nanowire nanosensors. *Nano Lett.* **2004**, *4*, 51-54.

(6) Cui, Y.; Wei, Q. Q.; Park, H. K.; Lieber, C. M. Nanowire nanosensors for highly sensitive and selective detection of biological and chemical species. *Science* **2001**, *293*, 1289-1292.

(7) Stern, E.; Vacic, A.; Rajan, N. K.; Criscione, J. M.; Park, J.; Ilic, B. R.; Mooney, D. J.; Reed, M. A.; Fahmy, T. M. Label-free biomarker detection from whole blood. *Nature nanotechnology* **2010**, *5*, 138-142.

(8) Xu, S. C.; Zhan, J.; Man, B. Y.; Jiang, S. Z.; Yue, W. W.; Gao, S. B.; Guo, C. G.; Liu, H. P.; Li, Z. H.; Wang, J. H.; Zhou, Y. Q. Real-time reliable determination of binding kinetics of DNA hybridization using a multi-channel graphene biosensor. *Nat Commun* **2017**, *8*.

(9) Tudos, A. J.; Besselink, G. A. J.; Schasfoort, R. B. M. Trends in miniaturized total analysis systems for point-of-care testing in clinical chemistry. *Lab on a chip* **2001**, *1*, 83-95.

(10) Mu, L. Y.; Droujinine, I. A.; Rajan, N. K.; Sawtelle, S. D.; Reed, M. A. Direct, Rapid, and Label-Free Detection of Enzyme Substrate Interactions in Physiological Buffers Using CMOS-Compatible Nanoribbon Sensors. *Nano Lett.* **2014**, *14*, 5315-5322.

(11) Kaisti, M. Detection principles of biological and chemical FET sensors. *Biosens. Bioelectron.* **2017**, *98*, 437-448.

(12) Bay, H. H.; Vo, R.; Dai, X. C.; Hsu, H. H.; Mo, Z. M.; Cao, S. R.; Li, W. Y.; Omenetto, F. G.; Jiang, X. C. Hydrogel Gate Graphene Field-Effect Transistors as Multiplexed Biosensors. *Nano Lett.* **2019**, *19*, 2620-2626.

(13) Gao, N.; Gao, T.; Yang, X.; Dai, X. C.; Zhou, W.; Zhang, A. Q.; Lieber, C. M. Specific detection of biomolecules in physiological solutions using graphene transistor biosensors. *Proc. Natl. Acad. Sci. U. S. A.* **2016**, *113*, 14633-14638.

(14) Chen, R. J.; Bangsaruntip, S.; Drouvalakis, K. A.; Kam, N. W. S.; Shim, M.; Li, Y. M.; Kim, W.; Utz, P. J.; Dai, H. J. Noncovalent functionalization of carbon nanotubes for highly specific electronic biosensors. *Proc. Natl. Acad. Sci. U. S. A.* **2003**, *100*, 4984-4989.

(15) Nakatsuka, N.; Yang, K. A.; Abendroth, J. M.; Cheung, K. M.; Xu, X.; Yang, H.; Zhao, C.; Zhu, B.; Rim, Y. S.; Yang, Y.; Weiss, P. S.; Stojanovic, M. N.; Andrews, A. M. Aptamer-field-effect transistors overcome Debye length limitations for small-molecule sensing. *Science* **2018**, *362*, 319-324.

(16) Stern, E.; Wagner, R.; Sigworth, F. J.; Breaker, R.; Fahmy, T. M.; Reed, M. A. Importance of the debye screening length on nanowire field effect transistor sensors. *Nano Lett.* **2007**, *7*, 3405-3409.

(17) Goode, J. A.; Rushworth, J. V. H.; Millner, P. A. Biosensor Regeneration: A Review of Common Techniques and Outcomes. *Langmuir* **2015**, *31*, 6267-6276.

(18) Pritchard, E. M.; Dennis, P. B.; Omenetto, F.; Naik, R. R.; Kaplan, D. L. Physical and chemical aspects of stabilization of compounds in silk. *Biopolymers* **2012**, *97*, 479-498.

(19) Bioactive hydrogels were functioanlized by incubating 40-50 μL of 100 μg/μL enzyme (penicillinase from Bacillus cererus and urease from Canavalia ensiformis, Sigma) solution with 40-50 μL of 100 μg/μL heterobifunctional PEG linker (Acrylate-PEG2K-NHS) (Sigma, JKA5021) for 1 h at room temperature. Solutions were prepared using 1X phosphate buffer saline (Gibco). PEGylated enzyme solution was mixed with PEGDA solution and Eosin Y disodium solution (5.0 mg/mL) with ratios of 50%,48.75%, and 1.25%, respectively.

(20) The 3D printed fluidic chamber was printed using Wanhao Duplicator 7 Desktop 3D Printer with Wanhao 3D-Printer UV Resin – Clear. After printing, the chamber was washed with ethanol and UV cured for 30 minutes. The chamber consists of several features for insertion of inlet/outlet tubing, mounting Ag/AgCl reference electrode and standard docking stations for aligning hydrogel stamp on top of FET device.

(21) Liu, Y. X.; Dong, X. C.; Chen, P. Biological and chemical sensors based on graphene materials. *Chem. Soc. Rev.* **2012**, *41*, 2283-2307.

(22) Ohno, Y.; Maehashi, K.; Yamashiro, Y.; Matsumoto, K. Electrolyte-Gated Graphene Field-Effect Transistors for Detecting pH Protein Adsorption. *Nano Lett.* **2009**, *9*, 3318-3322.

(23) Phosphate buffer solution was made by dissolving sodium phosphate dibasic (Sigma) and monobasic potassium phosphate (Sigma) in deionized water and adjusted pH to 7.4. Analyte solutions were prepared by dissolving various concentrations of penicillin G sodium salt (Sigma, 13752) or urea (Sigma, U0631) in the buffer solution.

(24) de Melo, J. V.; Cosnier, S.; Mousty, C.; Martelet, C.; Jaffrezic-Renault, N. Urea biosensors based on immobilization of urease into two oppositely charged clays (Laponite and Zn-Al layered double hydroxides). *Anal. Chem.* **2002**, *74*, 4037-4043.

(25) Russell, R. J.; Axel, A. C.; Shields, K. L.; Pishko, M. V. Mass transfer in rapidly photopolymerized poly(ethylene glycol) hydrogels used for chemical sensing. *Polymer* **2001**, *42*, 4893-4901.

(26) Lieleg, O.; Ribbeck, K. Biological hydrogels as selective diffusion barriers. *Trends Cell Biol.* **2011**, *21*, 543-551.

(27) Hoffman, A. S. Hydrogels for biomedical applications. *Adv. Drug Del. Rev.* **2002**, *54*, 3-12.

(28) Noshadi, I.; Hong, S.; Sullivan, K. E.; Sani, E. S.; Portillo-Lara, R.; Tamayol, A.; Shin, S. R.; Gao, A. E.; Stoppel, W. L.; Black, L. D.; Khademhosseini, A.; Annabi, N. In vitro and in vivo analysis of visible light crosslinkable gelatin methacryloyl (GelMA) hydrogels. *Biomater Sci-Uk* **2017**, *5*, 2093-2105.

(29) Lee, K. Y.; Mooney, D. J. Alginate: Properties and biomedical applications. *Prog. Polym. Sci.* **2012**, *37*, 106-126.

(30) The gelatin hydrogel monomer solution was made by mixing 10% (w/v) GelMA (Sigma, 900741) in deionized water with co-initiators 1-vinyl-2-pyrrolidinone 99% (VP) (Sigma, 201-800-4) and triethanolamine (TEA) (Sigma, 90279) with ratios of 77.45%, 15.15% and 7.40% w/v, respectively. Alginate hydrogel was made by mixing 3% alginate with 0.2 mM $CaCl_2$.

(31) Badiger, M. V.; Mcneill, M. E.; Graham, N. B. Porogens in the Preparation of Microporous Hydrogels Based on Poly(Ethylene Oxides). *Biomaterials* **1993**, *14*, 1059-1063.

(32) Delaney, J. T.; Liberski, A. R.; Perelaer, J.; Schubert, U. S. Reactive inkjet printing of calcium alginate hydrogel porogens-a new strategy to open-pore structured matrices with controlled geometry. *Soft Matter* **2010**, *6*, 866-869.

(33) Yuk, H.; Lu, B. Y.; Zhao, X. H. Hydrogel bioelectronics. *Chem. Soc. Rev.* **2019**, *48*, 1642-1667.

(34) Grigoryan, B.; Paulsen, S. J.; Corbett, D. C.; Sazer, D. W.; Fortin, C. L.; Zaita, A. J.; Greenfield, P. T.; Calafat, N. J.; Gounley, J. P.; Ta, A. H.; Johansson, F.; Randles, A.; Rosenkrantz, J. E.; Louis-Rosenberg, J. D.; Galie, P. A.; Stevens, K. R.; Miller, J. S. Multivascular networks and functional intravascular topologies within biocompatible hydrogels. *Science* **2019**, *364*, 458-464.

(35) 3D printed "stamps" and complementary PDMS well master mold were printed using Wanhao Duplicator 7 Desktop 3D Printer with Wanhao 3D-Printer UV Resin – Clear. After printing, the componenets were washed with ethanol and UV cured for 30 and 240 minutes, respectively. PDMS well dimensions were designed to fit uniformly with stamps. PDMS was casted onto the master mold and cured overnight at 70 °C. After casting, PDMS was removed from the mold and rendered hydrophillic by oxygen plasma etching (60 W for 1 min).

(36) Tanaka, T.; SWISLOW, G.; Ohmine, I. Phase-Separation and Gelation in Gelatin Gels. *Phys. Rev. Lett.* **1979**, *42*, 1556-1559.

(37) Kuchler, A.; Yoshimoto, M.; Luginbuhl, S.; Mavelli, F.; Walde, P. Enzymatic reactions in confined environments. *Nature nanotechnology* **2016**, *11*, 409-420.

(38) Liu, Q. J.; Wu, C. S.; Cai, H.; Hu, N.; Zhou, J.; Wang, P. Cell-Based Biosensors and Their Application in Biomedicine. *Chem. Rev.* **2014**, *114*, 6423-6461.

(39) Pham, T. D.; Pham, P. Q.; Li, J.; Letai, A. G.; Wallace, D. C.; Burke, P. J. Cristae remodeling causes acidification detected by integrated graphene sensor during mitochondrial outer membrane permeabilization. *Sci. Rep.* **2016**, *6*, 35907.

(40) Zhang, A.; Lieber, C. M. Nano-Bioelectronics. *Chem. Rev.* **2016**, *116*, 215-257.

(41) Zhou, W.; Dai, X. C.; Lieber, C. M. Advances in nanowire bioelectronics. *Rep. Prog. Phys.* **2016**, *80*, 016701.

(42) Dai, X. C.; Hong, G. S.; Gao, T.; Lieber, C. M. Mesh Nanoelectronics: Seamless Integration of Electronics with Tissues. *Acc. Chem. Res.* **2018**, *51*, 309-318.